Stacking disorder in silicon carbide supported cobalt crystallites: an X-ray diffraction, electron diffraction and high resolution electron microscopy study

H. E. du Plessis *[a], J. P. R. de Villiers [b], A. Tuling [b] and E. J. Olivier [c]

[a]Sasol Group Technology, Sasolburg, South Africa. E-mail: esna.duplessis@sasol.com
[b]University of Pretoria, Pretoria, South Africa
[c]Nelson Mandela Metropolitan University, Port Elizabeth, South Africa

Supported cobalt Fischer–Tropsch catalysts are characteristically nanoparticulate and the reduced SiC supported catalyst was found to contain both HCP and FCC polymorphs. This is reflected in the powder XRD patterns and generally there is a poor fit between the experimental and calculated diffractograms. This was ascribed to small crystallite sizes and the occurrence of disorder, manifested as peak broadening and peak shifts. Selected area electron diffraction data of suitably oriented cobalt catalyst grains on silicon carbide supports show non-periodic disorder in the zone axis orientations that contain the common (001) (HCP) and (111) (FCC) reciprocal lattice planes. Both FCC and HCP polymorphs are present in the same grains and these show disorder mainly in the HCP component. The disorder is further examined using high angle annular dark field (HAADF) scanning transmission electron microscopy at atomic resolution and the stacking sequences elucidated. Random sequences of mainly FCC are interrupted by HCP sequences and twin surfaces with reverse stacking sequences are also present. This study highlights the presence of significant disorder in cobalt catalyst grains confirmed by HAADF microscopy.

Introduction

Alumina supported cobalt catalysts are used in commercial Fischer–Tropsch synthesis (FTS) processes and a comprehensive review of advances in the development of cobalt catalysts is given in the paper by Khodakov et al.[1] A porous β-SiC supported FTS catalyst was reported to be stable in hydrothermally demanding environments.[2] The discussion of the activity of FCC cobalt in comparison with the HCP structure is also relevant. According to several investigators,[3–5] the HCP polymorph is more active than FCC cobalt. It is also well known that several stacking variations occur especially in metallic cobalt,[6,7] but their occurrence in catalysts and the influence of the various structure types and disorder on catalytic activity are not yet fully understood or documented.

In a study of the kinetics of the FCC to HCP transformation in pure cobalt, Zhao and Notis[8] showed that in addition to the common FCC and HCP polymorphs (denoted as α and ε, respectively) there are two other polymorphs that form during cooling at different rates. With relatively slow cooling (10 °C s^{-1}), an ε′ martensite forms with a postulated 4H structure, and with fast cooling (5×10^3 °C s^{-1}) an ε″ martensite forms with a 9R structure. However, Kajiwara et al.[9] reported that the 4H structure is not stable in fine particles at room temperature, and only the 2H (HCP) and 9R structures were found. Dinega and Bawendi[10]

described another polymorph (also called ε-cobalt) with a P4₁32 space group formed by the decomposition of $Co_2(CO)_8$.

Stacking disorder in cobalt in both fine-grained and quenched solid ingots has been comprehensively studied by Kajiwara in several publications.[9,11,12] In addition, the 9R cobalt structure in fine grained samples is described in detail.[11] A method to measure stacking fault probabilities on the basis of peak displacement in selected area diffraction patterns was developed by Kajiwara.

Aberration corrected high-resolution transmission electron microscopy, especially in the HAADF mode, is a relatively new development. Recent advances in the resolution of transmission microscopes have enabled the direct imaging of stacking sequences and stacking disorder. The direct imaging of the change in the stacking disorder of a Co–Cu alloy by Nakano et al.[13] is an example of the relation between the disorder shown by the SAD pattern and the direct image of the structure.

The aim of this contribution is to measure disorder in cobalt nanoparticles, deposited on silicon carbide using the procedure described by Labuschagne et al.[2] The catalyst was reduced, unloaded from the reactor and characterized. To study the effect of oxidative conditions in the hydrothermally challenging FTS reaction, the reduced catalyst was exposed to an oxidative thermal treatment (250 °C, 5 hours in air at atmospheric pressure), re-reduced and unloaded in air under ambient conditions for characterization.

The catalysts were characterized by powder X-ray diffraction (XRD), selected area electron diffraction (SAED), and high resolution transmission electron microscopy (HRTEM). The disorder in metallic cobalt was quantified by recording high resolution images.

Experimental procedure

The following samples were studied:

Reference cobalt Co

A reference cobalt metal standard was obtained from Sigma-Aldrich.

Reference catalyst CAT1

Co_3O_4 was supported on β-SiC (containing 13 wt% Co) using the procedure described by Labuschagne et al.[2]

Reduced catalysts R1 and R2

Catalysts R1 and R2 were prepared by repeated reductions of the reference catalyst CAT1 in a H_2 atmosphere whilst increasing the temperature from 25 °C to 550 °C at a rate of 1 °C min⁻¹ with an isothermal period of 4 hours at 550 °C. The experiments were performed at atmospheric pressure. Catalyst R1 was prepared to study the catalyst in the reduced state using TEM, whilst catalyst R2 was prepared as the starting material for the ROR1 catalyst.

Reduced, oxidized and reduced catalyst ROR1

To study the effect of oxidative conditions the reduced catalyst (R2) was exposed to an oxidative thermal treatment (250 °C, 5 hours in air at atmospheric pressure), re-reduced and characterized.

XRD analyses

The catalysts were reduced using in situ powder XRD in an XRK650 Anton Paar reaction chamber connected to a PANalytical X'Pert Pro Multipurpose diffractometer. The powder X-ray diffractograms of the reference Co, CAT1 and unloaded catalysts were measured from top-loaded poly-crystalline powders using a sealed cobalt tube source (λ K_α = 1.79031 Å), at 23 ± 1 °C.

The software X'Pert Highscore Plus© was used for phase identification and Topas4© was used for the average crystallite size analysis applying the fundamental parameter approach. The amorphous content of the catalyst prior to reduction was determined by addition of fluorite as an internal standard as described by Madsen et al.[14] The presence of amorphous material in a β-SiC supported cobalt catalyst was described by Labuschagne et al.[2]

TEM analyses

TEM studies were conducted to establish the presence of stacking disorder in the metallic phase. The samples were dispersed in ethanol, and the finest fraction was deposited on carbon films supported on copper microscope grids. The grids containing the cobalt particles were then carbon coated to prevent dislodgement of the magnetic particles. A Philips CM200 electron microscope was operated at 160 kV in bright field, dark field and selected area diffraction modes.

The metal samples were difficult to image at high resolution because of excessive absorption of the electron beam and the relatively large particle sizes of the cobalt grains. Selected area electron diffraction is particularly valuable in that the disorder is manifested in the diffraction pattern as streaking between single crystal diffraction spots. This streaking however is only visible in diffraction patterns that contain the stacking direction which is [111] for FCC cobalt and [0001] for HCP cobalt.

This means that a large number of crystallites must be identified and tilted to get crystallographic zone axes parallel to the electron beam. Most crystallites will be oriented along inappropriate zone axes and cannot be used to establish whether disorder is present or not.

The JEMS programme[15] was used for the indexing of the diffraction patterns. High resolution transmission electron microscopy was conducted on the same samples using a double aberration corrected JEOL ARM200F operated at 200 kV. Imaging was done in HAADF scanning transmission mode using a beam current of 68 pA and a probe size of approximately 0.1 nm. The convergence angle of the probe used was 24–27 mrad and the acceptance angles of the HAADF detector were from 68 to 280 mrad.

Results

Reference cobalt Co

The powder X-ray diffractogram obtained from the Sigma Aldrich sample (Fig. 1) contains both FCC and HCP cobalt. Rietveld analysis shows the peak shifts in especially the HCP polymorph. This is due to the presence of stacking disorder, as described by Kajiwara[9] which will be examined further in the discussion.
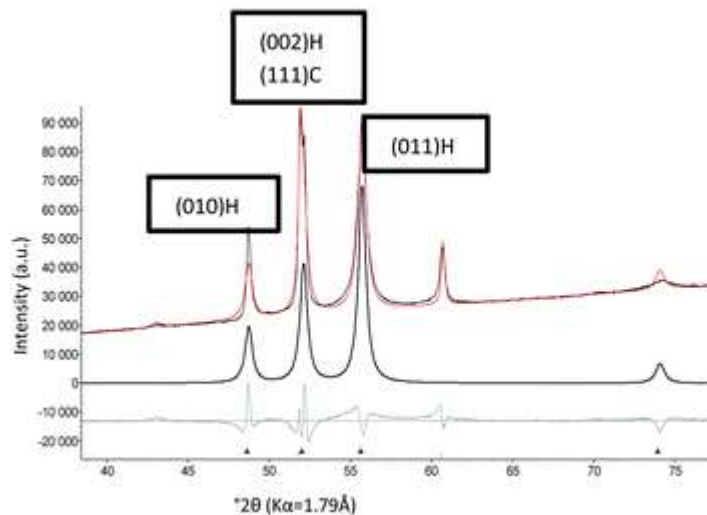

Fig. 1 X-ray diffractogram of Sigma-Aldrich cobalt (experimental top pattern). The (002) and (111) reflections of HCP (H) and FCC (C) cobalt denote the common stacking direction. The middle pattern is the calculated diffractogram of HCP cobalt, and the lower one is the difference between the calculated and experimental patterns.

A slight difference in the d-spacing between the hexagonal (002) and cubic (111), resulting in a split peak is also apparent.

Rietveld refinement was done by minimizing the difference between the theoretical powder diffractograms of the FCC and HCP cobalt structures published by Kohlhaas[16] and Owen[17] and the experimental diffractogram.

The reference cobalt contained 34(0.2)% FCC and 66(0.2) HCP cobalt with volume weighted average crystallite sizes of 28(0.4) nm and 14(0.1) nm, respectively. Analysis of the cobalt standard by transmission electron microscopy established the presence of disorder (Fig. 2). The specific crystal appears to consist solely of HCP cobalt.
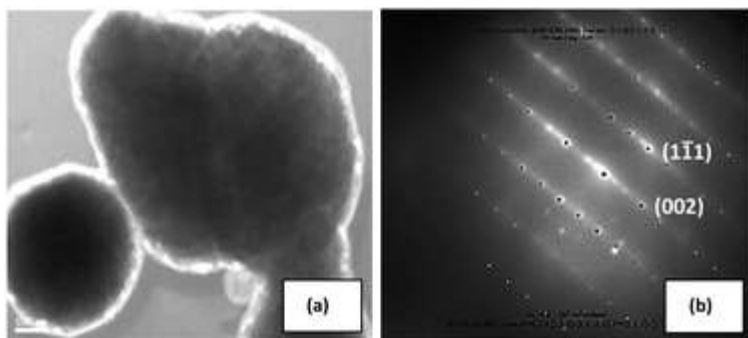
Fig. 2 (a) TEM image of a Co crystallite from Sigma-Aldrich with (b) its selected area diffraction pattern showing a disordering along the [00l] direction. Indexing is done on the basis of the HCP structure and the [110] zone axis is parallel to the electron beam.

Reference catalyst CAT1

Rietveld refinement indicated the catalyst to contain 18(0.5)% cobalt oxide spinel (Co_3O_4), 78(0.6)% β-SiC and 4(1)% amorphous silica. The average crystallite sizes of these phases were 19(0.2) nm and 32(0.8) nm. TEM analysis of the reference catalyst CAT1 showed small crystallites of cubic Co_3O_4 deposited on the SiC surfaces, Fig. 3(a).
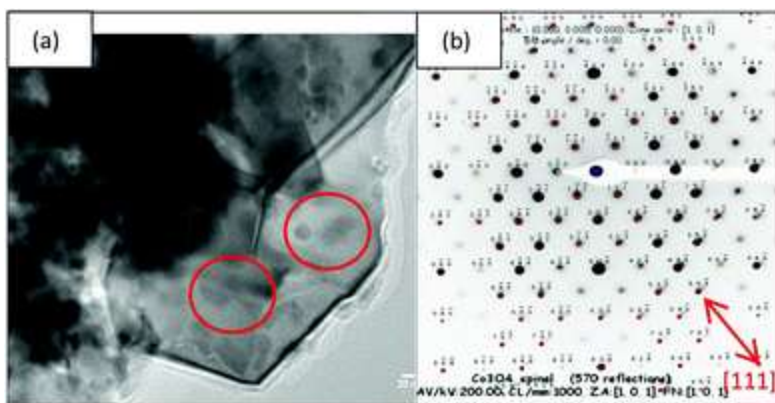

Fig. 3 (a) Small darker crystallites of Co_3O_4 deposited on β-SiC crystal surfaces (circles) and (b) indexed SAD pattern of another crystal of Co_3O_4 showing the absence of disorder (streaks) along the close-packed direction, [111], as indicated.

The Co_3O_4 crystallites were examined for the presence of disorder. No evidence of any disorder could be found as is shown in the [110] zone axis of the selected area diffraction pattern in Fig. 3(b).

Reduced catalysts R1 and R2

Part of the powder X-ray diffractogram of the reduced catalyst R1 (which is dominated by the support β-SiC reflections) is given in Fig. 4. It is clear that the FCC reflections are sharper than those from HCP cobalt. This is ascribed both to a smaller crystallite size of HCP cobalt and to the presence of strain (caused by disorder) in HCP cobalt.
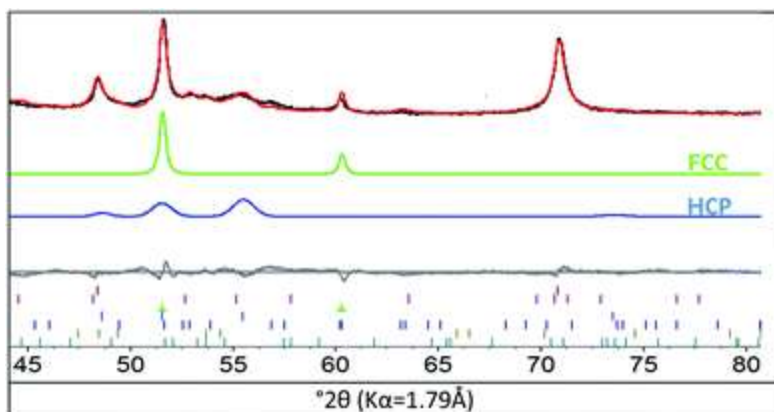
5

Fig. 4 A selected portion of the observed XRD pattern of cobalt on a SiC substrate (black) with the superimposed calculated pattern (red). The peaks in the calculated FCC diffractogram (green) are much sharper than those of HCP cobalt (blue). The difference pattern is shown at the bottom and the reflection at 71° 2θ is from the SiC substrate. The calculated patterns are obtained by Rietveld refinement.

The Rietveld refinement results confirmed that catalyst R1 contained 5(0.1)% FCC and 13(0.3)% HCP cobalt in addition to 4(0.3)% Co_2Si, with the remainder being β-SiC. These results compare well with those of catalyst R2: 6(0.1)% FCC and 12(0.3)% HCP cobalt and 3(0.3)% Co_2Si. The volume weighted average crystallite sizes of the phases were: 26(0.7) nm (FCC cobalt), 15(2) nm (HCP cobalt) and 15(1) nm Co_2Si. The HCP crystallites are significantly smaller than the FCC cobalt crystallites, resulting in broader peaks from the HCP phase, (see Fig. 4).

In catalyst R1, the electron diffraction pattern consists of diffraction spots from both FCC and HCP cobalt. Streaking found in diffraction spots originated from the HCP phase. This indicates the presence of thin plate-like features interrupting the regular structure (stacking faults). The absence of such streaking associated with the FCC reflections shows that this type of disorder is only present within the HCP regions of the crystals. This is shown in Fig. 5(a) and (b).
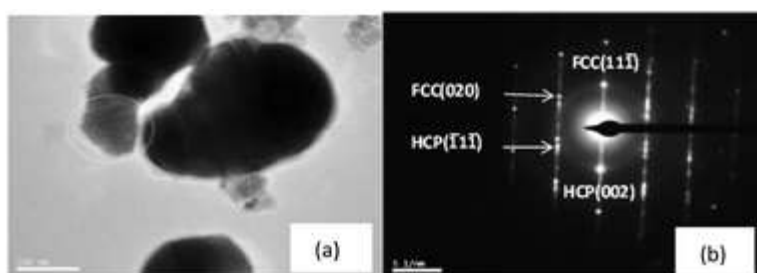

Fig. 5 (a) A Co particle with associated selected area diffraction pattern (b) showing the streaking associated with the HCP diffraction spots whilst the FCC spots are sharp and do not have associated streaking. The FCC (11$\bar{1}$) and HCP (002) reflections coincide.

The indexed FCC diffraction pattern in Fig. 5(b) shows the FCC diffraction spots to be discrete, while the streaks are associated with the HCP diffraction spots. This indicates that in the crystals examined, disorder in HCP cobalt is common, in contrast to FCC cobalt. This finding is supported by the X-ray diffractograms which show sharp FCC peaks in contrast to broadened HCP peaks.

Kajiwara[9] examined stacking disorder in cobalt and its alloys and derived a method to measure the stacking fault probabilities on the basis of the shifts of the electron diffraction spots along the $h - k = 3n + 1$ and $h - k = 3n - 1$ reciprocal lattice rows. These shifts are however very small, and attempts to measure them in suitable experimental diffraction patterns were unsuccessful due to the limited resolution of the diffraction patterns.

Another crystallite shows the same distribution of diffraction spots due to the presence of both FCC and HCP. This is shown in Fig. 6 where the images originating from the various diffraction spots are shown. The images from channels 3 and 4 as labelled in the diffraction pattern clearly show different domains in the crystallite. Some domains are highly disordered, whereas other domains in the same crystallite are relatively homogeneous with little disorder.
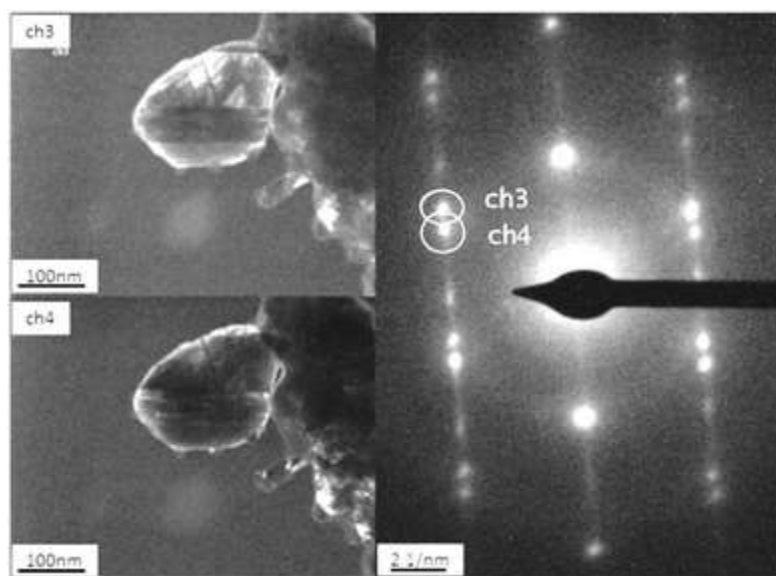

Fig. 6 Dark field images originating from different diffraction spots of the diffraction pattern. Channels 3 and 4 are from the FCC and HCP diffraction spots, respectively. Domains are clearly visible in the crystallite, but the proximity of the FCC and HCP diffraction spots cause some interference in the images.

The presence of Co_2Si in the reduced catalysts is not surprising and has been reported by Seng and Barnes.[18] Co_2Si was not formed during the preparation of the Co_3O_4/β-SiC catalyst since the phase forms by the reaction of metallic cobalt with the SiC support. The reduced catalysts however contain Co_2Si as it was formed during the reduction process:

$$SiC + 2Co \rightarrow Co_2Si + C$$
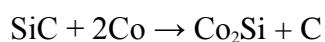
Reduced, oxidized and reduced catalyst ROR1

To study the effect of oxidative conditions on the catalyst the reduced catalyst (R2) was exposed to an oxidative thermal treatment (250 °C, 5 hours in air at atmospheric pressure), re-reduced and characterized. Quantitative phase analyses indicated the ROR1 catalyst to contain 5(0.2)% FCC and 7(0.5)% HCP cobalt, 4(0.6)% Co_2Si and 2(0.5)% CoO. The volume weighted average crystallite sizes were: 13(0.5) nm FCC and 3(0.3) nm HCP cobalt, 6(0.9) nm Co_2Si and 4(1) nm CoO.

The cobalt monoxide phase consists of small crystallites (4 nm) and FCC cobalt consists of smaller crystallites than originally present in the R1 catalyst (FCC was 26(0.7) nm in R1, now 13(0.5) nm). This indicates the formation of an oxide passivation layer during unloading the ROR1 catalyst from the reactor. The ROR1 catalyst contained an abundance of Co_2Si similar to the R1 and R2 catalysts.

The average crystallite size of FCC cobalt in the ROR1 catalyst is significantly smaller than that in the R1 and R2 catalysts. This points to re-dispersion of metallic cobalt, frequently observed during recycling of supported metal catalysts.[19]

In this catalyst sample, (Fig. 7), selected area diffraction shows the occurrence of diffraction spots from both the FCC and HCP phases. This observation implies that both polymorphs are present in most of the crystallites examined by TEM.
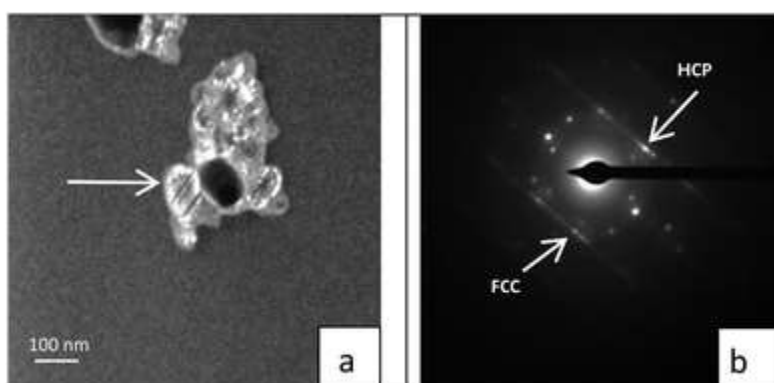

Fig. 7 (a) Dark field image of a crystallite (see arrow) from ROR1 showing stacking faults oriented along the stacking direction of both FCC and HCP cobalt. (b) Diffraction pattern of the crystallite shown in (a). The diffraction pattern is indistinct due to the small size of the crystallite.

The dark field image in (a) shows the presence of planar defects that could be associated with the disorder. This is imaged at higher resolution in successive images.

High resolution transmission electron microscopy images of the metallic cobalt particles were obtained. Fig. 8 shows a metallic cobalt crystallite with an oxide rim at the top.

The cobalt particle consists of a domain containing numerous stacking faults and another that is relatively homogeneous, similar to the particle in Fig. 7.

This shows unequivocally that both faulted and un-faulted regions can co-exist in the same particle. Again, it is postulated that the un-faulted region consists of FCC cobalt.

In order to elucidate the stacking sequences in cobalt, a high resolution image of a faulted particle was collected. This is shown in Fig. 9.
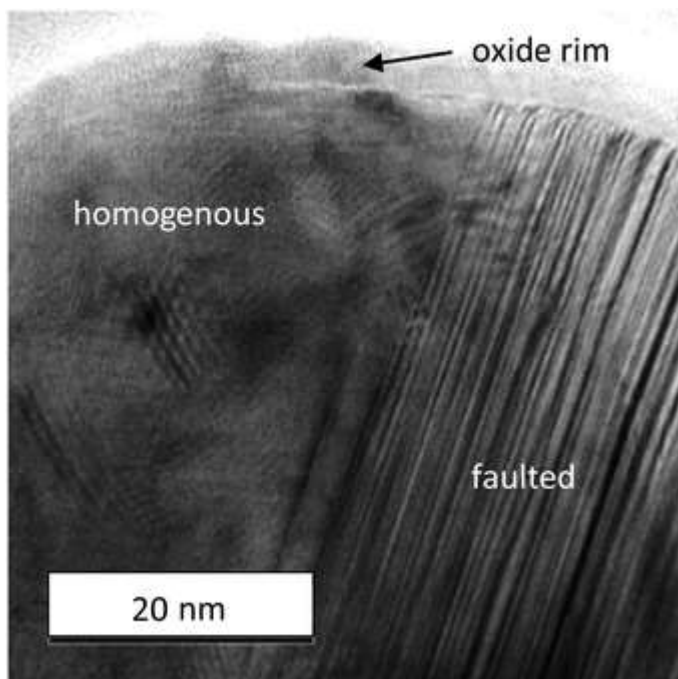
Fig. 8 High resolution BF STEM image showing both faulted (right) and homogeneous regions (left) in cobalt. An oxide rim is visible at the top of the image.
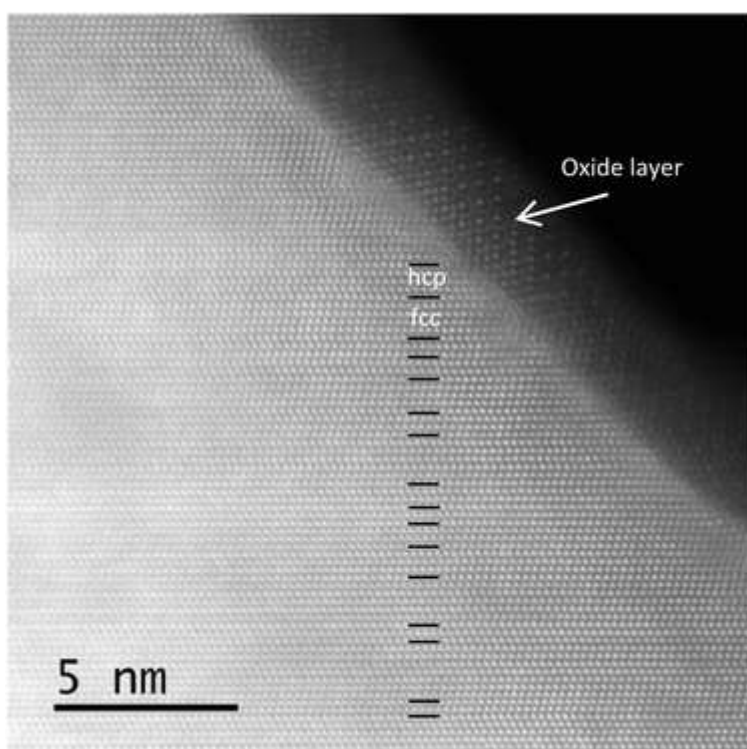

Fig. 9 HAADF STEM image of a faulted cobalt crystallite showing some of the numerous non-periodic stacking sequences. An oxide layer is present at the particle edge (top right).

As can be seen in the figure, numerous non-periodic stacking sequences are visible, some not so easy to decipher. Wider regions having FCC stacking (ABCABC) are interrupted by smaller HCP (ABAB) layers. Again, an oxide layer is present at the surface of the grain. The epitaxy between cobalt and cobalt oxide is also visible.

Measurement of stacking disorder

The disorder was elucidated by recording HAADF STEM images and matching them with computed HAADF images of the pure HCP and FCC phases. An analysis of the frequency of the HCP and FCC phases as well as a large number of stacking faults was performed on three HAADF images (Fig. 10 shows one of the images). These represent the number of rows (FCC or HCP) in high resolution images that have been measured. A large variability in stacking faults are present in the different images, giving rise to the variability in the results in Table 1, which gives the estimates of stacking percentages.
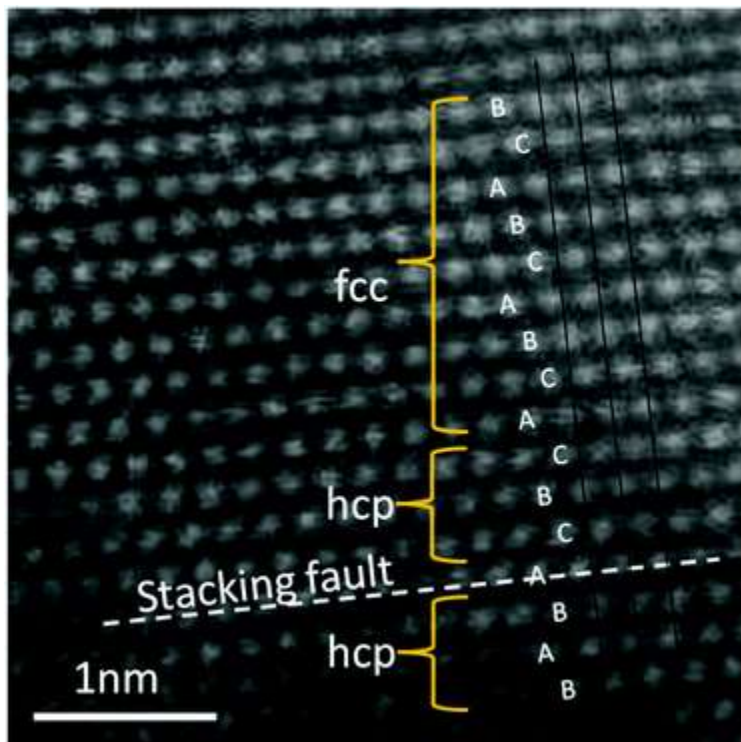

Fig. 10 HAADF image with the interpreted FCC and HCP stacking sequences.

Table 1 Estimates of percentage FCC and HCP as well as stacking faults in three HAADF images

Number of rows	%FCC	%HCP	%SF	Twin planes in FCC
66	64	27	9	0
62	63	32	5	8
79	87	10	3	11

It shows that FCC is the dominant phase, with the amount of stacking faults less than 10%. The actual stacking fault figure in the bulk material may be much less as TEM is a selective technique (only a few crystals are studied).

Conclusions

This study has confirmed the presence of non-periodic stacking disorder in cobalt catalyst particles by the use of powder X-ray diffraction analysis, selected area electron diffraction and high resolution transmission electron microscopy. Streaking along the close packing directions of SAD patterns is the confirmation of the non-periodic disorder, and this seems to be confined to the HCP polymorph only.

The high resolution images provide experimental confirmation of the presence of stacking faults in cobalt catalysts. Stacking faults were observed in all the Co-containing phases in the catalyst series: reduced Co/β-SiC (R1 and R2) and ROR-treated Co/β-SiC catalysts (ROR1). These faulted metallic cobalt crystals may affect the Fischer–Tropsch synthesis activity of the catalyst under hydrothermally challenging conditions. This also highlights the difference between crystallite and particle sizes in that single particles can contain domains of both FCC and HCP crystallites.

Because of the highly selective nature of normal and high-resolution electron microscopy, a more appropriate method is needed to study and quantify the amount of stacking faults in bulk catalysts. If faulted crystallites are indeed affecting the catalyst behaviour, then X-ray diffraction methods as described by Longo et al.[7] could be better used to characterise cobalt catalysts. These are under investigation at present. Comparison with the microscopic results will only be possible once these studies have been performed on the same catalyst samples.

Acknowledgements

References

1. A. Y. Khodakov, W. Chu and P. Fongerland, Chem. Rev., 2007, **107**, 1692
2. J. Labuschagne, R. Meyer, Z. H. Chonco, J. M. Botha and D. J. Moodley, Catal. Today, 2016, **275**, 2 .
3. O. Ducreux, B. Rebours, J. Lynch, M. Roy-Auberger and D. Bazin, Oil Gas Sci. Technol., 2009, **64**(1), 49
4. M. Sadegzadeh, H. Karaca, O. V. Safonova, P. Fongarland, S. Chambrey, P. Roussel, A. Griboval-Constant, M. Lacroix, D. Curulla-Ferré, F. Luck and A. Y. Khodakov, Catal. Today, 2011, **16**4, 62
5. V. A. De la Pena O'Shea, P. R. de la Pischina, N. Homs, G. Aromi and J. L. G. Fierro, Chem. Mater., 2009, **21**, 5637 .
6. A. Y. Babkevich, F. Frey, V. Gramlich and W. Steurer, Phys. Status Solidi, 1996, **154**, 517
7. A. Longo, L. Sciortino, F. Giannici and A. J. Martorana, Appl. Crystallogr., 2014, **47**, 1562
8. J. C. Zhao and M. R. Notis, Scr. Metall. Mater., 1995, **32**(10), 1671
9. S. Kajiwara, S. Ohno and K. Honma, Philos. Mag., 1991, **63**(4), 625
10. D. P. Dinega and M. G. Bawendi, Angew. Chem., Int. Ed., 1991, **38**(12), 1788
11. S. Kajiwara, Jpn. J. Appl. Phys., 1970, **9**(4), 385
12. S. Kajiwara, S. Ohno, K. Honma and M. Uda, Philos. Mag. Lett., 1987, **55**(5), 215
13. H. Nakano, M. Yuasa and M. Mabuchi, Scr. Mater., 2009, **61**, 371
14. I. C. Madsen, N. V. Y. Scarlett and A. Kern, Z. Kristallogr., 2011, **226**, 944
15. P. Stadelmann, Microsc. Microanal., 2003, **9**(S03), 60
16. R. Kohlhaas, P. Duenner and N. Schmitz-Pranghe, Fiz. Met. Metalloved., 1968, **26**, 140
17. E. A. Owen and J. Madoc, Proc. Phys. Soc., 1954, **67**, 459
18. W. F. Seng and P. A. Barnes, Mat. Sci. Eng., 2000, **B76**, 225
19. K. Morgan, A. Goguet and C. Hardacre, ACS Catal., 2015, **5**(6), 3430